JULY 1975 MATT-1142

PARAMETRIC INSTABILITIES AND ANOMALOUS DIFFUSION NEAR THE UPPER-HYBRID FREQUENCY

BY

L. CHEN AND H. OKUDA

PLASMA PHYSICS LABORATORY

PRINCETON UNIVERSITY
PRINCETON, NEW JERSEY

This work was supported by U. S. Atomic Energy Commission Contract AT(11-1)-3073. Reproduction, translation, publication, use, and disposal, in whole or in part, by or for the United States Government is permitted.

DISCLAIMER

Parametric Instabilities and Anomalous Diffusion Near the Upper-Hybrid Frequency

Liu Chen and Hideo Okuda
Plasma Physics Laboratory, Princeton University
Princeton, New Jersey 08540

ABSTRACT

Parametric instabilities and associated anomalous particle diffusions due to a pump oscillating near the upper-hybrid frequency are studied in theory and by numerical simulations for a two-dimensional magnetized plasma. It is shown that, besides the three-wave decay process, the convective-cell mode, a purely damped diffusive mode in the absence of pump, can be parametrically driven to be a purely growing mode. Accompanied with the enhanced fluctuations, anomalous particle diffusion is observed. Theory and simulation results are in good agreement.

I. INTRODUCTION

Recently, there has been considerable interest in parametric instabilities excited in plasmas with regard to rf plasma heating and laser-plasma interactions. In this work, we present theoretical and numerical simulation results of parametric instabilities excited in a magnetized plasma by an external pump oscillating near the upper-hybrid frequency. Previous authors have considered similar parametric processes.[1-3] We find, however, a new parametric instability which involves the coupling to the convective-cell mode.[4] As will be shown in the simulation results, parametric excitation of the convective-cell mode results in enhanced particle cross-field diffusion.

In the absence of pump, the convective-cell mode, a diffusive mode, is associated with the vortex motion of charged particles across the magnetic field. It is nonoscillatory and purely damped by ion viscosity. Simulations[4] have shown that this mode plays a significant role in particle cross-field diffusion even in thermal equilibrium; especially, in plasmas with a relatively strong magnetic field; i.e., $\omega_{pe} \lesssim \omega_{ce}$. ω_{pe} and ω_{ce} are, respectively, electron plasma and cyclotron frequencies. One, therefore, would expect anomalous particle cross-field diffusion to take place if the energy of this mode is enhanced above the thermal level. In the following sections, we show that the convective-cell mode can, indeed, be parametrically driven to be unstable (more specifically, purely growing) and cause anomalous diffusion.

Theory of parametric instability associated with the convective-cell mode is presented in Section II. In Section III, we present numerical simulation results to compare with the theory. Simulation results also show the three-wave decay process discussed in Ref. 1. Conclusions and discussions are given in Section IV.

II. THEORY OF PARAMETRIC EXCITATION OF CONVECTIVE-CELL MODE

We assume the plasma to be infinite, spatially homogeneous, and uniformly magnetized with $\underset{\sim}{B}_o = B_o \underset{\sim}{e}_z$. The external electromagnetic pump is assumed to be uniform in space (dipole approximation) with its oscillating electric field $\underset{\sim}{E}_o$ perpendicular to $\underset{\sim}{B}_o$; that is,

$$\underset{\sim}{E}_o = E_o \cos(\omega_o t)\, \underset{\sim}{e}_x ,$$

where $\omega_o \sim \omega_{uh}$ is the pump frequency. $\omega_{uh} = (\omega_{pe}^2 + \omega_{ce}^2)^{1/2}$ is the upper-hybrid frequency.

To analyze the parametric excitations of electrostatic waves due to $\underset{\sim}{E}_o$, we use the standard technique of transforming the electron Vlasov and Poisson equations to the electron oscillating frame[2,5] and obtain the following dispersion relation describing the coupling between the low-frequency (ω) , upper-sideband ($\omega + \omega_o$) , lower-sideband ($\omega - \omega_o$) and the pump (ω_o) modes. Here, $|\omega| << \omega_o$ throughout this work.

$$\left(\frac{1}{\chi_i^o} + \frac{1}{\varepsilon_e^o}\right)\left[1 + \frac{\lambda_e^2}{4}\left(\frac{1}{\varepsilon_e^+} + \frac{1}{\varepsilon_e^-}\right)\right] + \frac{\lambda_e^2}{4}\left(\frac{1}{\varepsilon_e^+} + \frac{1}{\varepsilon_e^-}\right)$$

$$+ \frac{\lambda_e^4}{4}\frac{1}{\varepsilon_e^+\varepsilon_e^-} = 0 \ . \qquad (1)$$

In Eq. (1), superscripts o , + , and - denote, respectively, the ω , $\omega + \omega_o$ and $\omega - \omega_o$ modes. To simplify the notations, dependences on the wave number $\underset{\sim}{k}$ are suppressed here. χ_i and χ_e are ion and electron linear susceptibilities, respectively. χ_i is obtained from the Braginskii set of fluid equations and, hence, includes the ion viscous effect.[4] $\varepsilon_e = 1 + \chi_e$ is the electron dielectric function. λ_e , the electron coupling coefficient, is related to electron displacement due to $\underset{\sim}{E}_o$ and is given by

$$\lambda_e = \frac{eE_o}{m_e\omega_o^2}\left(1 - \frac{\omega_{ce}^2}{\omega_o^2}\right)^{-1}\left(k_x^2 + k_y^2\frac{\omega_{ce}^2}{\omega_o^2}\right)^{1/2} \ . \qquad (2)$$

λ_i is $O(m_e/m_i)$ smaller than λ_e and is, therefore, ignored here. In deriving Eq. (1), we have assumed the pump is weak; i.e., $|\lambda_e| < 1$. $O(\lambda_e^4)$ term must be included here, because $\varepsilon_e^o \sim O(1)$ for $\underset{\sim}{k} \perp \underset{\sim}{B}_o$ and, therefore, $\lambda_e^2/\varepsilon_e^{\pm}$ is generally of order unity.

We are interested in electrostatic waves with $\underset{\sim}{k} \perp \underset{\sim}{B}_o$ and $k_\perp\rho_i < 1$; ρ_i being ion Larmor radius. Note for $T_e \sim T_i$,

ρ_e (electron Larmor radius) $<<$ ρ_i . For $|\omega| < \omega_{ci}$ and $\omega_o = \omega_{uh} + \delta$ ($|\delta| << \omega_{uh}$) , the χ's and ε's are then approximately[4]

$$\chi_e^o = \chi_e(\omega) \simeq \omega_{pe}^2/\omega_{ce}^2 \quad , \tag{3}$$

$$\chi_i^o = \chi_i(\omega) \simeq \frac{\omega_{pi}^2}{\omega_{ci}^2} \frac{\omega + i\mu_i}{\omega} \quad , \tag{4}$$

$$\varepsilon_e^{\pm} = \varepsilon_e(\omega \pm \omega_o) \simeq (\partial\varepsilon_e^r/\partial\omega_{uh})[\delta \pm (\omega + i\nu_e)] \quad , \tag{5}$$

where

$$\partial\varepsilon_e^r/\partial\omega_{uh} \simeq 2\omega_{uh}/\omega_{pe}^2 \quad . \tag{6}$$

In the above expressions, μ_i denotes the ion viscous effect; $\mu_i \simeq \nu_{ii} k_\perp^2 \rho_i^2$ and ν_{ii} is the ion-ion collision frequency.[4] Since $\mu_i >> \mu_e$, electron viscous effect can be neglected here. ν_e is the electron-ion collision frequency. Substituting Eqs. (3) to (6) into Eq. (1), we have with $\omega = iy$

$$y^3 + \Gamma_o y^2 + \Gamma_1 y + \mu_i \Gamma_2 = 0 \quad , \tag{7}$$

where

$$\Gamma_o = 2\nu_e + \alpha\mu_i/(\alpha + \beta) \ , \tag{8}$$

$$\Gamma_1 = \left[(\alpha + \beta)\left(K\delta + \delta^2 + \nu_e^2\right) + K\delta + K^2 + 2\alpha\nu_e\mu_i \right]/(\alpha + \beta) \ , \tag{9}$$

$$\Gamma_2 = \left[\alpha\left(K\delta + \delta^2 + \nu_e^2\right) + K\delta + K^2\right]/(\alpha + \beta) \ , \tag{10}$$

$$K = \lambda_e^2\omega_{pe}^2/4\omega_{uh} \ , \tag{11}$$

$$\alpha = \left(1 + \omega_{pe}^2/\omega_{ce}^2\right)^{-1} < 1 \ , \tag{12}$$

and

$$\beta = \omega_{ci}^2/\omega_{pi}^2 \ . \tag{13}$$

Since $\nu_e >> \mu_i$, Γ_o and Γ_1 can be simplified to

$$\Gamma_o \simeq 2\nu_e \ , \tag{8'}$$

$$\Gamma_1 \simeq \Gamma_2 + \beta\left(K\delta + \delta^2 + \nu_e^2\right)/(\alpha + \beta) \ . \tag{9'}$$

The low-frequency mode of interest here is the convective-cell mode. Thus, $|y| \sim O(\mu_i) << \nu_e$, we can then neglect the y^3 and y^2 terms in Eq. (7) and obtain the following solution

$$y \simeq - \mu_i \Gamma_2 / \Gamma_1 \ . \tag{14}$$

Since Γ_1 and Γ_2 are real, the mode is nonoscillatory, being either purely damped or purely growing.

The threshold condition is given by $\Gamma_2 = 0$, or

$$K_c^2 + \delta(\alpha + 1)K_c + \alpha\left(\delta^2 + \nu_e^2\right) = 0 \ . \tag{15}$$

Because K_c , $\alpha > 0$, Eq. (15) can be satisfied only when

$$\delta = - |\delta| < 0 \ . \tag{16}$$

With δ being negative, Eq. (15) then has two solutions K_1 and K_2 ;

$$K_1 = \left[|\delta|(1 + \alpha) - \left(\delta^2(1 - \alpha)^2 - 4\alpha\nu_e^2\right)^{1/2} \right] /2 \ , \tag{17}$$

$$K_2 = \left[|\delta|(1 + \alpha) + \left(\delta^2(1 - \alpha)^2 - 4\alpha\nu_e^2\right)^{1/2} \right] /2 \ . \tag{18}$$

Note here that real solutions of K_1 and K_2 exist and $0 < K_1 \leq K_2$ for $|\delta| \geq 2\alpha^{1/2}\nu_e/(1 - \alpha)$. The minimum threshold, K_m , occurs at

$$|\delta|_m = (1 + \alpha)\nu_e/(1 - \alpha) \ , \tag{19}$$

and

$$K_m = 2\alpha\nu_e/(1 - \alpha) \ . \tag{20}$$

For $K_1 < K < K_2$, $\Gamma_2 < 0$ and one has $y \geq 0$; i.e., a purely growing solution, if $\Gamma_1 > 0$. It follows from Eq. (9') that $\Gamma_1 > 0$ if $\beta (= \omega_{ci}^2/\omega_{pi}^2)$ is sufficiently large and/or K is close to the threshold values. Near the threshold, let $K = K_{1,2}(1 \pm p)$ and $p < 1$, the growth rate is given by

$$\omega \simeq ip\mu_i \ |\delta|(1 + \alpha)\alpha/[\beta(|\delta| - k_{1,2})] \ . \tag{21}$$

Here, $|\delta| - K_{1,2}$ is always positive. We have also solved Eq. (7) numerically and obtained good agreement with the above analytical results for the $\omega \sim O(\mu_i)$ solution.

Since the low-frequency mode of this instability is non-oscillatory and is of transport time scale, $|\omega| \sim O(\mu_i) << \omega_{ci}$, it can be expected that the excitation of this mode would cause anomalous particle diffusion. Both the excitation and the associated anomalous diffusion are observed in numerical simulations to be discussed in the next section.

As $|\omega|$ becomes much larger than μ_i , this purely growing mode goes over to the oscillating-two-stream instability discussed by McBride.[2] Furthermore, as shown by Tzoar,[1] there are also

three-way decay processes; such as upper-hybrid and lower-hybrid modes as well as Bernstein modes. For $k_\perp \rho_e \lesssim 1$, however, the upper-hybrid and lower-hybrid decay process is predicted to be the dominant one. This is confirmed in the simulations.

III. RESULTS OF NUMERICAL SIMULATION

In this section, results from numerical simulations will be presented and comparisons made with the theory given in the preceding section. The simulation model is an electrostatic two-dimensional dipole expansion code with periodic boundary conditions. The uniform external magnetic field is in the z-direction. Grid sizes in x- and y-directions are equal and taken to be the units of spatial scales. Time scales are in unit of ω_{pe}^{-1} .

Since the growth rate is proportional to ν_{ii} , we use a small number of particles per cell to enhance the growth rate in order to facilitate the simulations. This, however, also enhances the value of ν_e and, from Eq. (20), raises the threshold pump value. The simulation parameters are

System size: 64 x 64 , Number of particles: 64 x 64 ,

$m_e/m_i = 1/25$, $T_e/T_i = 1$,

$\omega_{ce}/\omega_{pe} = \sqrt{2}$, $\Delta t = 0.25$,

$\lambda_{De} = 1$; Particle size = 2 ,

$\rho_e = 0.71$, $\rho_i = 3.54$.

Corresponding to these parameters, we have

$$\omega_{ci}/\omega_{pi} = 0.28 \ , \ \omega_{uh} = 1.73 \ \omega_{pe} \ ,$$

$$\omega_{\ell h} = \omega_{pi}\left(1 + \omega_{pe}^2/\omega_{ce}^2\right)^{-1/2} = 0.173 \ .$$

ν_e , the electron-ion collision frequency, is in the order of $10^{-3}\ \omega_{pe}$. Initially, particles are randomly loaded with Maxwellian velocity distributions. The external pump electric field is of the form

$$\underset{\sim}{E}_o = E_o \cos\ (\omega_o t)\ \underset{\sim}{e}_x \ , \tag{22}$$

where

$$\omega_o = 1.74\ \omega_{pe} \ , \tag{23}$$

and

$$\varepsilon_o E_o^2/nT_e(0) = 0.747 \ . \tag{24}$$

This $\underset{\sim}{E}_o$, for example, corresponds to $\lambda_e^2(1,0) \simeq 7.5 \times 10^{-3}$ or $K(1,0) \simeq 1.1 \times 10^{-3}$ for the (1,0) mode. Since the initial fluctuations have finite frequency bandwidths (Figs. 4 and 5), and, due to the finite length of simulation runs, the pump also has a finite frequency resolution $\Delta\omega \sim 2\pi/T$, it is found

that the excitation is relatively insensitive to the frequency mismatch $\delta = \omega_o - \omega_{uh}$ as long as $|\delta|$ is smaller than the frequency spread. We have tried both the $\delta = 0.01\ \omega_{pe}$ and $\delta = -0.01\ \omega_{pe}$ cases, the results obtained are essentially the same. The $\delta = 0.01\ \omega_{pe}$, i.e., $\omega_o = 1.74\ \omega_{pe}$, case is presented here.

Figure 1 shows the time evolution of total field energy normalized with respect to the initial thermal energy for both the pumped and no pump cases. Without pump, the normalized field energy fluctuates about the 0.01 value. With pump, however, the field energy increases with time more or less exponentially. The measured growth rate is approximately $3.4 \times 10^{-4}\ \omega_{pe}$. Throughout the entire run to $\omega_{pe}t = 10^3$, no tendency of saturation is observed.

In Figs. 2 and 3, electron and ion guiding center diffusion in the x-direction are plotted for both the pumped and no pump cases. Only $\langle(\Delta x)^2\rangle$ is plotted here because $\langle(\Delta y)^2\rangle \simeq \langle(\Delta x^2)\rangle$. It is apparent from these plots that the parametric instability causes anomalous particle diffusion of both electrons and ions. The anomalous electron diffusion coefficient is measured to be $D_e^* \simeq 0.37$, which is about a factor of three larger than the thermal-equilibrium value, $D_e \simeq 0.11$. For ions the anomalous diffusion coefficient $D_i^* \simeq 0.27$ is also roughly a factor of three larger than the thermal-equilibrium value, $D_i \simeq 0.08$. The anomaly factor can grow further since the instability has not saturated yet.

In order to understand the physics more clearly, we have also analyzed and compared the power spectra for both the pumped and no pump cases. The results for the long-wavelength, (1,0) , mode and the relatively shorter-wavelength, (2,3) , mode are, respectively, shown in Figs. 4 and 5. As noted in the preceding section, the peaks in the thermal spectra have finite widths. For the (1,0) mode, there is a large enhancement, about a factor of sixty, in the mode energy near $\omega = 0$, which corresponds to the convective-cell mode. There are also enhancements near the lower-hybrid frequency. Corresponding to the enhancement in the convective-cell mode, there is enhancement in the upper-hybrid mode near $\pm \omega_o$. This shows that the convective-cell mode is parametrically excited as predicted by the theory. The few scattered points near $\omega \simeq 1.57$ may correspond to the enhancements in the lower-hybrid mode. This upper-hybrid and lower-hybrid decay instability is clearly indicated in the power spectrum of the (2,3) mode shown in Fig. 5. Again, there are enhancements in the convective-cell and lower-hybrid modes. The enhancements in the upper-hybrid, however, exhibit two peaks. One is near $\pm \omega_o$ and indicates the convective-cell parametric instability. The other peak is near $\omega \simeq \pm 1.57$ and corresponds to the enhancement resulted from the upper-hybrid and lower-hybrid decay instability.

Because most of the field energy is in the long-wavelength modes where the dominant parametric instability mechanism is associated with the convective-cell mode, we can roughly compare the growth rate with the theoretically predicted value which is of order of μ_i , the ion viscous damping rate. If we take the

measured ion thermal-equilibrium diffusion coefficient D_i and let $\mu_i = k^2 D_i$ for the (1,0) mode, we obtain $\mu_i \approx 8 \times 10^{-4}\ \omega_{pe}$, which is about only a factor of two different from the measured growth rate, $\gamma = 3.4 \times 10^{-4}\ \omega_{pe}$. That D_e^* is larger than D_i^* is understandable because lower-hybrid mode is also enhanced by the decay process.

IV. CONCLUSIONS AND DISCUSSIONS

In the previous sections, we have shown both by theory and numerical simulations, that the convective-cell mode can be parametrically excited to be a purely growing mode by an external pump oscillating near the upper-hybrid frequency. As a result of this parametric instability, energy of the convective-cell mode is enhanced and anomalous cross-field diffusion of electrons and ions are observed. The observed growth rate agrees reasonably well with the theoretical estimate. Simulation results also show the decay instability of the upper-hybrid and lower-hybrid waves as theoretically predicted by Tzoar.[1]

Since rf waves with frequencies near the upper-hybrid frequency are still under active consideration in laboratory plasma heating experiments, such as electron cyclotron resonance heating (ECRH) experiments, the results presented in this work indicate the possibility that in such experiments convective-cell modes can be parametrically driven to be unstable and may cause anomalous particle diffusion.

Although we have only considered here the case where the pump frequency is near the upper-hybrid frequency and the excited waves have $\underset{\sim}{k} \perp \underset{\sim}{B}_o$, it can be expected that similar parametric processes can take place in other frequency regimes when there is appreciable energy available associated with the convective-cell mode.

The plasma treated in this work is assumed to be uniform in space. In reality, the plasma has spatial nonuniformities in both density and temperature. These nonuniformities not only modify the properties of low-frequency waves[6] but also introduce wave vector mismatches in the parametric processes.[7] Investigations in these phenomena remain to be carried out.

ACKNOWLEDGMENTS

The authors are thankful to A. Hasegawa for initial inspirations to this work.

This work was supported by United States Energy Research and Development Administration (formerly AEC) Contract E(11-1)-3073.

REFERENCES

[1] N. Tzoar, Phys. Rev. 178, 356 (1969).

[2] J. B. McBride, Phys. Fluids 13, 2725 (1970).

[3] J. A. Fejer and E. Leer, Radio Sci. 7, 481 (1972).

[4] H. Okuda and J. M. Dawson, Phys. Fluids 16, 408 (1973).

[5] J. Sanmartin, Phys. Fluids 13, 1533 (1970).

[6] J. Canosa, J. A. Krommes, C. Oberman, H. Okuda, K. Tsang, J. M. Dawson, and T. Kamimura, IAEA-CN-33/H2 (1974), Fifth Conference on Plasma Physics and Controlled Nuclear Fusion, Tokyo, Japan.

[7] M. N. Rosenbluth, Phys. Rev. Lett. 31, 203 (1973).

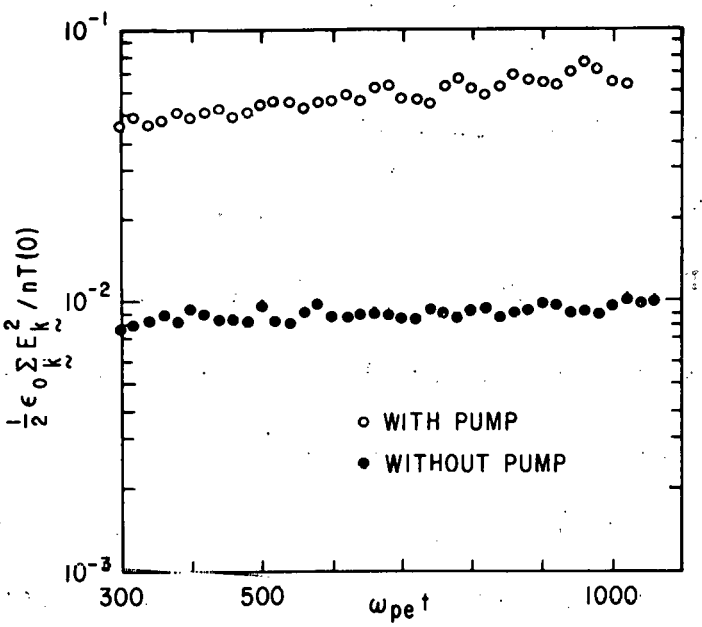

752087

Fig. 1. Plot of the normalized total field energies with time for the pumped and no pump cases. Initial transient states to the thermal noise level are not shown here.

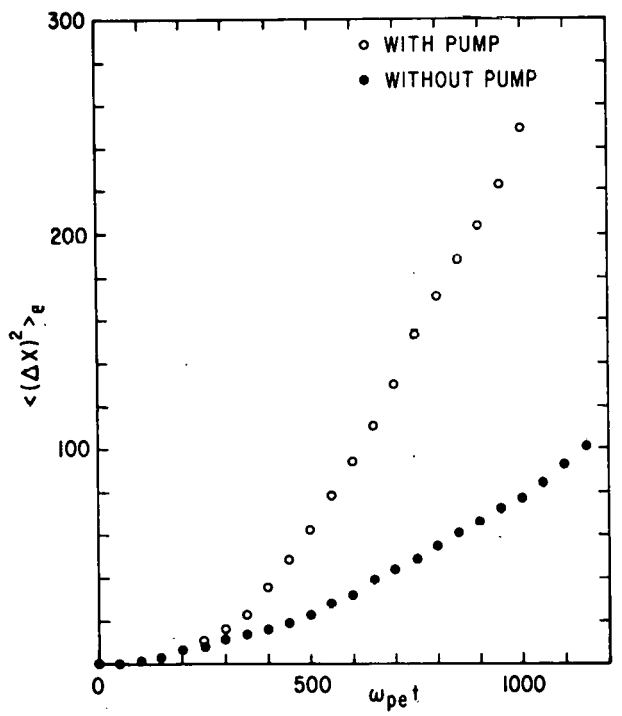

752088

Fig. 2. Plot of the squares of the guiding center displacement in x-direction for the test electrons with time for the pumped and no pump cases.

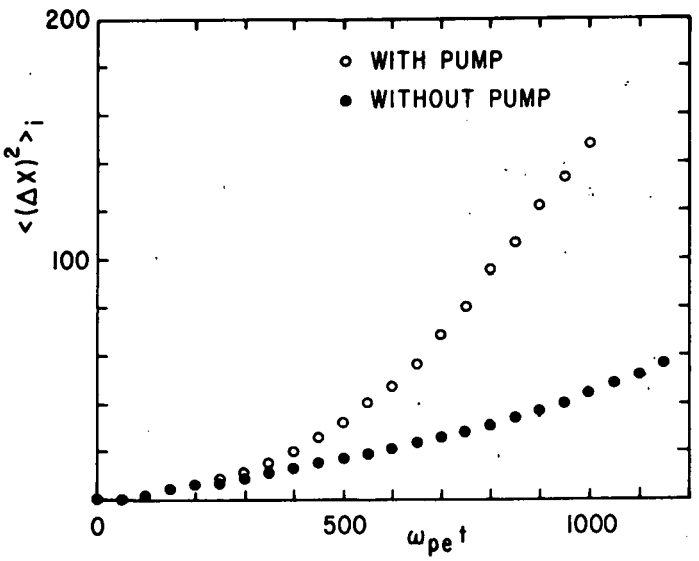

752089

Fig. 3. Plot of the squares of the guiding center displacement in x-direction for the test ions with time for the pumped and no pump cases.

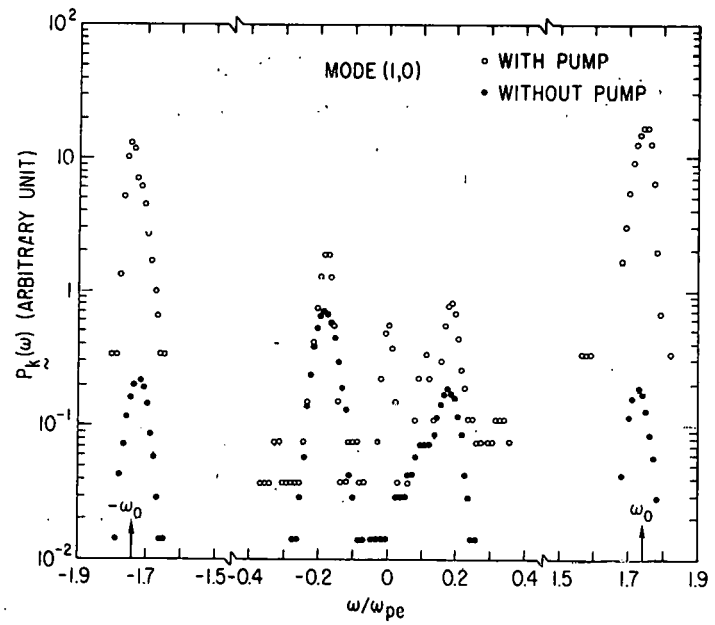

752090

Fig. 4. Power spectra of the electrostatic potential for the (1,0) mode with and without the pump wave.

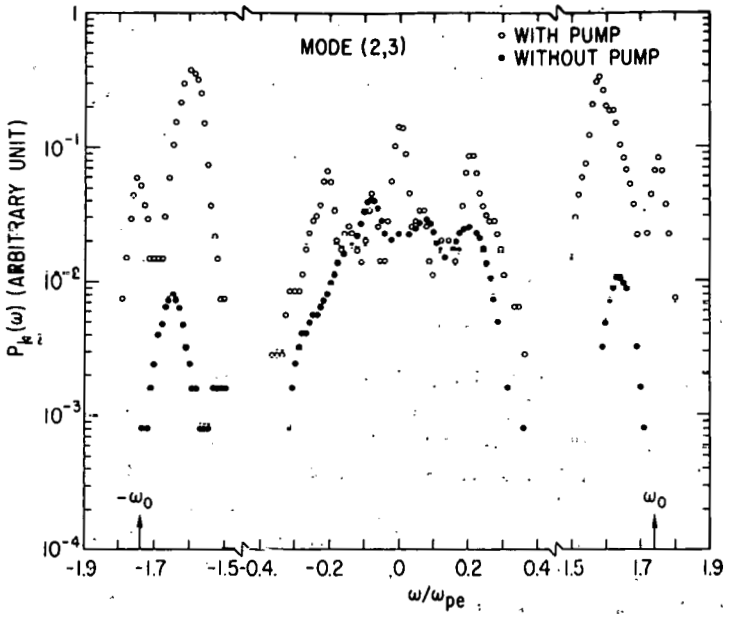

752091

Fig. 5. Power spectra of the electrostatic potential for the (2,3) mode with and without the pump wave.